



A comparison of neutral and charged species of one- and two-dimensional models of graphene nanoribbons using multireference theory

Shawn Horn and Hans Lischka

Citation: *The Journal of Chemical Physics* **142**, 054302 (2015); doi: 10.1063/1.4906540

View online: <http://dx.doi.org/10.1063/1.4906540>

View Table of Contents: <http://scitation.aip.org/content/aip/journal/jcp/142/5?ver=pdfcov>

Published by the AIP Publishing

Articles you may be interested in

Bond length and electric current oscillation of long linear carbon chains: Density functional theory, MpB model, and quantum spin transport studies

J. Chem. Phys. **140**, 134703 (2014); 10.1063/1.4869858

Electrical control of the spin polarization of a current in “pure-carbon” systems based on partially hydrogenated graphene nanoribbon

J. Appl. Phys. **113**, 244302 (2013); 10.1063/1.4811716

Electronic properties of graphene nanoribbons stacked on boron nitride nanoribbons

J. Appl. Phys. **113**, 133701 (2013); 10.1063/1.4798593

Electronic structure and transport properties of sulfur-passivated graphene nanoribbons

J. Appl. Phys. **112**, 113710 (2012); 10.1063/1.4768524

Analytical models of approximations for wave functions and energy dispersion in zigzag graphene nanoribbons

J. Appl. Phys. **111**, 074318 (2012); 10.1063/1.3702429

An advertisement for AIP Applied Physics Reviews. It features a blue and orange background with a central graphic of a molecular structure. The text "NEW Special Topic Sections" is prominently displayed in white. To the left, there is a thumbnail image of a journal cover for "AIP Applied Physics Reviews". The journal cover shows a 3D rendering of a nanowire or similar structure. Below the main text, it says "NOW ONLINE" and "Lithium Niobate Properties and Applications: Reviews of Emerging Trends". The AIP logo is at the bottom right.

A comparison of neutral and charged species of one- and two-dimensional models of graphene nanoribbons using multireference theory

Shawn Horn¹ and Hans Lischka^{1,2,a)}

¹Department of Chemistry and Biochemistry, Texas Tech University, Lubbock, Texas 79409-1061, USA

²Institute for Theoretical Chemistry, University of Vienna, Wahringerstrasse 17, 1090 Vienna, Austria

(Received 4 December 2014; accepted 12 January 2015; published online 2 February 2015)

This study examines the dependence of the polyyradical character of charged quasi-linear *n*-acenes and two-dimensional periacenes used as models for graphene nanoribbons in comparison to the corresponding neutral compounds. For this purpose, high-level *ab initio* calculations have been performed using the multireference averaged quadratic coupled cluster theory. Vertical ionization energies and electron affinities have been computed. Systematic tests show that the dependence on chain length of these quantities can be obtained from a consideration of the π system only and that remaining contributions coming from the σ orbitals or extended basis sets remain fairly constant. Using best estimate values, the experimental values for the ionization energy of the acene series can be reproduced within 0.1 eV and the experimental electron affinities within 0.4 V. The analysis of the natural orbital occupations and related unpaired electron densities shows that the ionic species exhibit a significant decrease in polyyradical character and thus an increased chemical stability as compared to the neutral state. © 2015 AIP Publishing LLC. [<http://dx.doi.org/10.1063/1.4906540>]

I. INTRODUCTION

Polycyclic aromatic hydrocarbons (PAHs) are found in nature as environmental pollutants¹ and are related to chemical reactivity of black carbon interfaces in soil.² Additionally, PAHs are found rather abundantly in the interstellar medium³ and are thought to be the cause of several unidentified bands in the mid-IR spectral range.^{4–6} Recently, PAHs have received increasing attraction as they are commonly used to model the electronic structure of graphene and graphene nanosheets.^{7,8} Graphene is a fascinating material and of great interest because of its potential use in nano-electronics.⁹ An important tool to tune the electronic properties of graphene is the introduction of defects.¹⁰ There are several means by which this goal can be achieved, which include chemical doping,¹¹ ejection of carbon atoms,¹² forming of ionic species, oxidation,¹³ and covering in surfactant.¹⁴

Of the PAHs, quasi-linear acenes (Scheme 1(a)) and two-dimensional nanoribbons (Scheme 1(b)) have been frequently used to investigate the amazing electronic properties of graphene. One remarkable feature of the mentioned PAHs is the high radical character at the zigzag edges,^{15–20} which leads, e.g., to a high chemical reactivity of the acenes with pentacene being the largest well-characterized acene.²¹

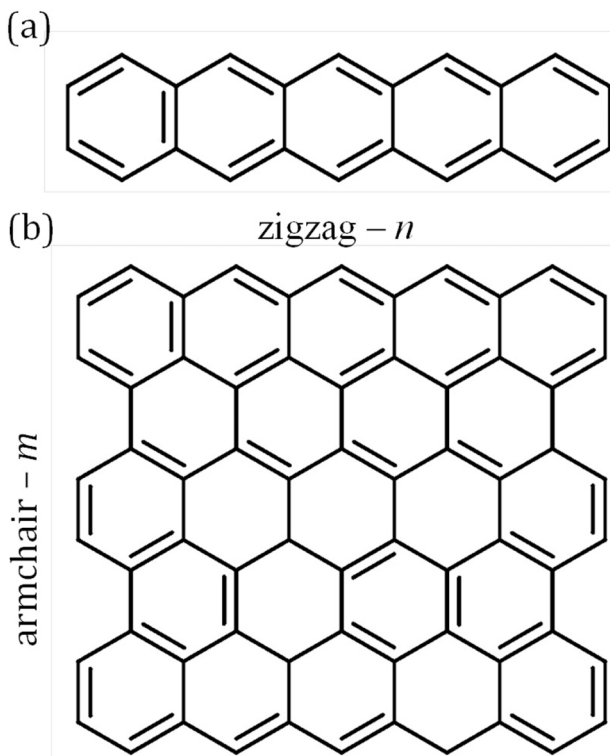
Forming charged species is an interesting way to alter the electronic structure of the PAHs. By the addition and removal of a single electron, an anion and cation, respectively, are formed for each of the molecular species. Many groups have concentrated on the energetic aspects by investigating electron affinities (EA) and ionization energies (IE) of PAHs. The ionization potentials of various members of the acene series have been measured with time-resolved photoioniza-

tion mass spectrometry,²² two-laser resonant photoionization mass spectrometry,²³ charge-stripping mass spectrometry,²⁴ and photoelectron spectroscopy.²⁵ The electron affinity of naphthalene was first reported by Burrow *et al.*²⁶ with the use of electron transmission spectroscopy. This technique captures the anionic energy for continuum states, which for the case of electronic ground states is only applicable in the acene series for benzene and naphthalene, as all the anionic acenes beyond that are more stable than their respective neutral ground states. Going beyond naphthalene, photodetachment photoelectron spectroscopy has been applied to anthracene at supercooled temperatures²⁷ and tetracene and pentacene have been investigated with an electron transfer equilibria technique.²⁸ To our knowledge, no experimental data are available for the periacene series.

In terms of theoretical studies, different versions of the outer valence Green's function (OVGF) method were used by Ohno *et al.*²⁹ to quantify the ionization potential bands of naphthalene and anthracene and by Ortiz *et al.*³⁰ to calculate those of anthracene and tetracene. The third-order algebraic diagrammatic construction (ADC(3)) method has been used³¹ to calculate the early shake-up potential bands of anthracene. Coupled cluster calculations with singles and doubles and non-iterative triples (CCSD(T)) have been performed by Deleuze *et al.*³² Although no theoretical data are available for the charged periacene species, some small 2D systems such as pyrene and chrysene have been investigated in Ref. 33 in which ADC(3) and OVGF methods have been used. The bulk of the previous theoretical work^{34–36} on anionic acenes has been performed at the density functional theory (DFT)³⁷ level. CCSD(T) calculations have been performed as well³⁷ for adiabatic electron affinities (AEAs).

Beyond the just-described ionization energies and electron affinities of selected PAHs, relatively little attention has

^{a)}E-mail: hans.lischka@univie.ac.at



SCHEME 1. Structures (a) *n*-acene and (b) (*ma*, *nz*) periacene.

been paid to the more general question of their electronic structure and in particular to their polyyradical nature. The goal of this work is to explore these properties in more detail by examining the singly ionic states of acenes and periacenes. It has already been mentioned at the beginning of this section that the neutral polyacenes and periacenes acquire substantial radical character with increasing chain length and that it is mostly concentrated at the zigzag edges. The focus of the present work is directed towards the question of how the electronic structure is affected by addition or removal of an electron and how, thereby, the polyyradical character and thus the chemical reactivity of the ionized species are changed in comparison to the corresponding neutral compounds. We have shown in previous work on singlet and triplet states of neutral polyacenes and periacenes^{18,38} that their polyyradical character can be well addressed by means of an *ab initio* multireference (MR) formalism. It is the purpose of this investigation to apply this approach also to the mentioned charged acenes and periacenes. The multireference method is based on a general concept aiming at an efficient representation of the electronic wavefunction by constructing a reference space containing the most important quasi-degenerate configurations (non-dynamical electron correlation) and representing the dynamical correlation by means of single and double excitations.³⁹ Size-extensivity contributions are included at the level of the multireference averaged quadratic coupled cluster (MR-AQCC)⁴⁰ approach, which has been successfully applied and found particularly useful for larger aromatic systems.^{18,38,41–44}

Based on the MR-AQCC calculations, analysis of the polyyradical nature of the acenes and periacenes is performed by two means: monitoring the evolution of the natural orbital (NO) occupation with increasing chain length and using

the effectively unpaired density. The latter method was first proposed by Takatsuka *et al.*⁴⁵ and was further developed by Staroverov and Davidson.⁴⁶ The methodology used in this paper comes from Head-Gordon.⁴⁷ Calculations employing the effects of polarized and diffuse basis sets on these quantities are considered as well for all the molecular systems.

II. COMPUTATIONAL DETAILS

The acenes (Scheme 1(a)) were examined from *n* = 2–8, *n* being the number of fused benzene rings in the chain. The periacenes (Scheme 1(b)) were studied from (3*a*,2*z*) to (3*a*,5*z*) in which the integers count the number of benzene rings along each direction, and *a* and *z* denote armchair and zigzag edges, respectively. These molecules belong to the D_{2h} symmetry group, with b_{1u} , b_{2g} , b_{3g} , and a_u being the irreducible representations that correspond to the π orbitals. The geometries for the acenes and periacenes were taken from Ref. 18, which had been optimized with second order Møller-Plesset perturbation theory⁴⁸ including the resolution of the identity approach (RI-MP2)^{49,50} with a SV(P) basis set.⁵¹ The orbital occupation scheme of the doubly occupied orbitals was obtained by performing a DFT calculation with the Becke-Perdew functional^{52,53} and a 6-31G(d) basis set. For the purposes of this study, the “zigzag” edge of the acenes and periacenes (Scheme 1) is taken to be along the x-axis in the x-y plane. DFT calculations were performed with the TURBOMOLE^{54,55} program package, and all other calculations used COLUMBUS.^{56–60}

Previous calculations on acenes^{18,38} had shown that large active spaces (up to 16 electrons in 16 orbitals) were necessary for producing reliable MR-AQCC calculations. A corresponding complete active space (CAS) with a reference space of that size would be far too large. Therefore, as an efficient compromise, a smaller CAS was chosen which was augmented by a restricted active space (RAS) and an auxiliary space (AUX). Four electrons were correlated in four orbitals to form the CAS and six orbitals were included in the AUX. AUX orbitals are obtained by moving virtual orbitals into the active space. An increasing number of RAS orbitals were included by including orbitals from the reference doubly occupied space as the size of the *n*-acenes increased (number of RAS orbitals equals *n* until *n* = 6, and remained at this value for *n* > 6). Only single excitations were allowed from the RAS and into the AUX space. This created a RAS/CAS(4,4)/AUX framework used for the multiconfiguration self-consistent field (MCSCF) calculations performed to determine the molecular orbitals (MOs). This RAS/CAS(4,4)/AUX was also used as a reference space in constructing a multireference expansion in configuration state functions (CSF) with all single and double excitations into the virtual orbital space.³⁹

The MR-AQCC method⁴⁰ already mentioned above was used for the calculations on the acenes. For the periacenes though, MR-AQCC calculations were not feasible due to a significant number of intruder states which led, in many cases, to non-converging calculations. Intruder states are defined as configurations not contained in the reference space which nevertheless acquire a significant weight. As threshold for that weight, a value of ~1% was adopted.

Extending the reference space to include these configurations turned out to be computationally too expensive. Therefore, in this case, the multireference configuration interaction with singles and doubles (MR-CISD) method was employed and a CAS(8,8) was chosen containing two orbitals for each of the symmetries of the π orbitals. To account for quadruple and higher excitations, the renormalized Davidson correction^{39,61} (denoted +Q) was used as follows:

$$E_Q = \frac{(1 - c_0^2)(E_{CI} - E_{REF})}{c_0^2} \quad (1)$$

in which c_0^2 is the sum of the squared coefficients of the reference configurations in the MR-CISD expansion and E_{REF} denotes the reference energy.

The requirements in terms of basis set were significantly more challenging especially for the anions as compared to the neutral systems investigated before.^{18,38} Because of the drastically enhanced computational requirements, extensive surveys of different factors influencing the results, such as basis set and freezing schemes for the σ orbitals, were performed to develop a procedure by which to compute the electron affinities and ionization energies for the larger acenes. As will be discussed below, the most extended calculations were performed for anthracene only, but the validity of the developed corrections in terms of basis sets and freezing of σ orbitals was verified by calculations on larger members of the acene series up to heptacene. For anthracene, a full scope of Pople⁶² basis sets was used ranging from 6-31G up to 6-311G(2d,f)^{63,64} with augmented functions for the carbon atoms. Augmentation here is performed by adding up to 2 diffuse functions to the s and p functions by scaling the lowest occurring exponent by a factor of 1/3 for each function added. The latter is denoted d-aug-6-311G(2d,f).⁶³ For the EA calculations of the remaining acenes, 6-31G, aug-6-31G, and aug-6-31G(d) basis sets were taken. Likewise, for the π IE calculations, 6-31G, 6-31G(d), and doubly polarized 6-31G (6-31G(2d)) were chosen. No difference was found between the π and the all valence calculations for IE; therefore, no σ - π correlation correction is included. Each of the basis sets listed above is that for carbon. For the hydrogen, only s basis functions are included for each respective basis set.

The MR-AQCC calculations correlating all valence electrons and using larger basis sets including especially double augmentation became excessively demanding for the systems beyond anthracene. Therefore, the most extended set of calculations, in terms of molecular size, were performed by freezing all σ orbitals. Starting from a self-consistent field (SCF) calculation, all occupied and virtual σ orbitals were frozen by transforming the one- and two-electron integrals into a new basis, keeping only the π orbitals. The effect of the frozen σ orbitals was folded into effective one-electron Hamilton matrix elements according to the formalism described by Shavitt.⁶⁵ This procedure resulted in a significant enhancement of the efficiency of the MCSCF and MR-AQCC calculations since only the π orbitals needed to be considered which decreased the effective basis set size considerably. For consistency with previous calculations,^{18,38} a closed-shell SCF representation was taken for all states of all species. For

comparison, σ orbitals derived from a series of restricted open-shell SCF calculations for the cations and anions and the 6-31G basis were used in the freezing scheme as well. The ionization energies did not change as compared to the use of the closed shell σ orbitals, but the electron affinities were increased on average by 0.31 eV for the acene series $n = 2\text{--}8$. Thus, in the case of π calculations, the value of 0.31 eV is included in the correction for the σ correlation. To test the σ freezing scheme, a second series of calculations (also using a 6-31G basis set) was performed where only the σ core orbitals were frozen. In these calculations though, a slightly smaller reference space was taken. Based on the comparison of the results of the calculations in the π only and the full valence space including the σ orbitals, a σ - π correlation correction (denoted as +TC in the figures—"Total Correction") is added to the EA π calculations. In this context, "Total" denotes the electron correlation treatment with the inclusion of all occupied π and valence σ orbitals.

Vertical ionization energy (VIE) and electron affinity (VEA) are computed as the difference of energies obtained by independent calculations with the neutral, cation, and anion at the optimized geometry of the neutral system. The electron affinity is defined as $EA = E_n - E_a$, in which E_n is the neutral state energy and E_a is the anionic energy. A negative EA value represents an unbound state. Ionization energy is calculated as $IE = E_c - E_n$ in which E_c is the cationic energy.

The effectively unpaired electron densities and total number of effectively unpaired electrons (N_U)^{45–47} were computed to discuss the polyyradical character of the different molecular systems. To avoid overemphasizing the contribution of the NOs that are nearly doubly occupied or nearly unoccupied, the non-linear model suggested in Ref. 47 was chosen, where N_U is given by

$$N_U = \sum_{i=1}^M n_i^2 (2 - n_i^2) \quad (2)$$

in which n_i is the occupation of the i th NO, and M is the number of NOs.

III. RESULTS

In the first part of this section, the calculations of the ionization energy and electron affinity of the n -acenes and of the periacenes will be presented. The second part will be dedicated to the discussion of the electronic structure of the singly positively and negatively charged n -acenes and of the periacenes with particular emphasis of their radical character and unpaired densities. The symmetries of the doublet states of these charged systems are found by removing one electron from the π system and adding one, respectively. The symmetry of the cationic and anionic states, respectively, depends on the symmetry of the highest occupied natural orbital (HONO) and the lowest occupied natural orbital (LUNO), respectively. For the neutral ${}^1\text{A}_g$ state, the symmetry of HONO for the acene and periacene series alternates between a_u and b_{2g} , and conversely, the LUNO symmetry alternates between b_{3g} and b_{1u} . Therefore, the computation of the lowest ionic state is reduced to an alternation between states (anion: ${}^2\text{B}_{3g}$ and

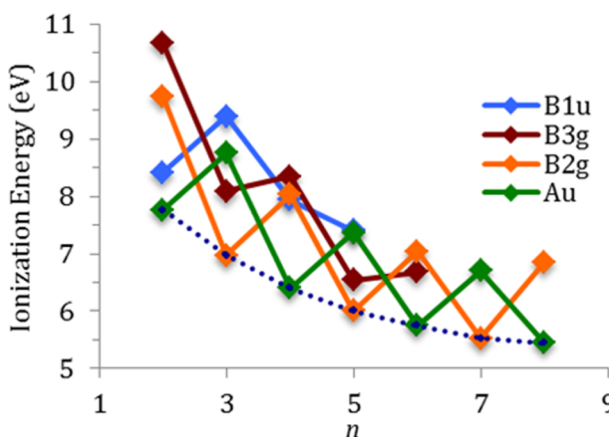


FIG. 1. First ionization energy for n -acenes ($n = 2-8$) with respect to the $^1\text{A}_\text{g}$ state using the π -MR-AQCC/RAS/CAS(4,4)/AUX/6-31G approach.

$^2\text{B}_{1\text{u}}$, cation: $^2\text{A}_\text{u}$ and $^2\text{B}_{2\text{g}}$). However, explicit calculations (see below) were made for all symmetries to check this assumption.

A. Ionization energy

The dotted line in Figure 1 (Table S1 in the supplementary material⁶⁶ contains these data in tabular form; the same procedure has been followed for other figures as well) indicates the alternation of the $^2\text{A}_\text{u}$ and $^2\text{B}_{2\text{g}}$ states as described above for the ionization energy. For the acene series (Figure 1), the two states that were never the lowest ($^2\text{B}_{3\text{g}}$ and $^2\text{B}_{1\text{u}}$) suffered from intruder states. Accordingly, some of the values, especially for the larger acenes, are not given.

Figure 2 (Table S2⁶⁶) shows MR-AQCC results obtained with more extended basis sets where only the energetically lowest state according to Figure 1 has been computed. A first comparison of the IE computed with the σ system frozen and with all valence electrons correlated (Figure 2, Table S2⁶⁶) using the 6-31G basis set shows that the latter calculation does not change the calculated ionization energy, as the two curves nearly perfectly overlay. A series of significantly larger basis sets was used for anthracene in order to create an incremental scheme for estimating basis set effects (Table I). The addition

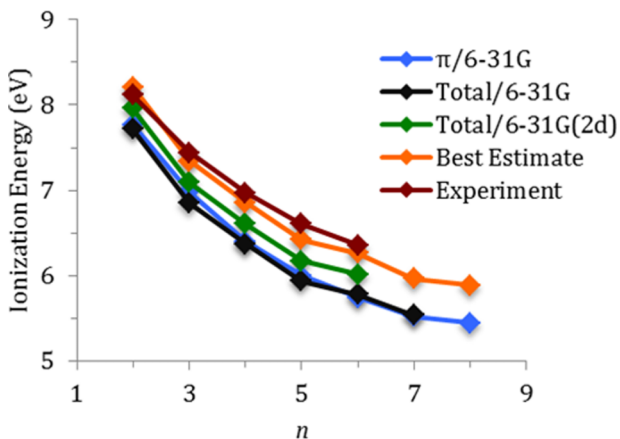


FIG. 2. First ionization energy for n -acenes ($n = 2-8$) for MR-AQCC using several basis sets in comparison with the experiment.²²⁻²⁵

TABLE I. Basis set comparison with experiment for ionization energy (eV) of all valence calculations of anthracene.

Basis set	IE
6-31G	6.85
6-31G(d)	7.00
6-31G(2d)	7.09
Aug-6-31G	7.06
d-aug-6-31G	7.06
d-aug-6-311G(d)	7.22
d-aug-6-311G(2d)	7.29
d-aug-6-311G(2d,f)	7.34
Experiment ^a	7.44

^aReference 23.

of a single polarization function (6-31G vs. 6-31G(d)) shows a 0.15 eV increase in the IE. Adding a second d function (6-31G(2d)) increases the IE by 0.09 eV. Independently, the addition of a single diffuse function to 6-31G (aug-6-31G) changes the IE by 0.21 eV. Extending the number of diffuse functions beyond the first one had a negligible effect (<0.01 eV).

Combining these functions and allowing for somewhat more flexibility in the valence part of the s and p bases, the use of the d-aug-6-311G(2d) leads to an increase of the computed ionization energy by 0.44 eV in relation to the 6-31G result. Adding an f function improves agreement with experiment to 0.10 eV. In summary, the improvements in the quality of the basis set with respect to the 6-31G basis amount to 0.49 eV. Table S2⁶⁶ shows that the basis set increment of 0.24 eV between the 6-31G(2d) and 6-31G results is very well constant up to $n = 6$, the largest calculated acene with the former basis set. Assuming such a behavior also for the more extended basis sets, the total increment of 0.49 eV is added to the total/6-31G IEs for the larger acenes. Thereby, the theoretical-experimental error is reduced to 0.12 ± 0.04 eV (shown as “Best Estimate” curve in Figure 2 and Table S2⁶⁶).

In view of the increased size of the periacenes and the experience with the calculations on the n -acenes concerning the insensitivity of the ionization energies to the inclusion of σ orbitals into the calculation, only π /MR-CISD+Q results have been performed for the periacenes (Figure 3, Table S3⁶⁶). In analogy to Figure 1 for the acenes, the dotted line in

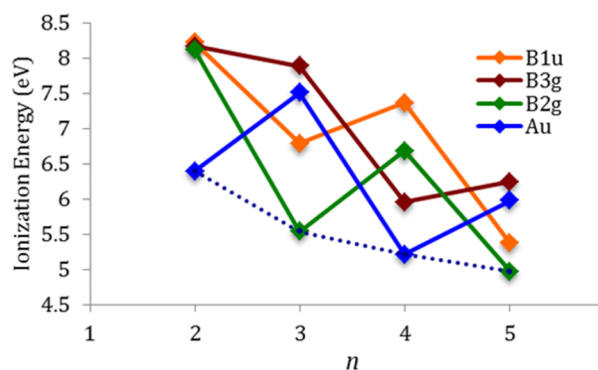


FIG. 3. First ionization energies for the $(3\text{a},\text{nz})$ periacenes ($n = 2-5$) using the π -MR-CISD/CAS(8,8)/6-31G approach.

Figure 3 shows, similar to the analysis found the acenes, the alternation of the 2A_u and $^2B_{2g}$ states for the ionization energy. A comparison of molecular systems of similar size between the acenes (Figure 2) and periacenes (Figure 3), such as 7-acene and (3a,3z) periacene, shows their *IEs* to be 5.52 eV and 5.54 eV, respectively, demonstrating an internal consistency within the calculations. Further wavefunction analysis, as examined in Sec. III C, will support the adequacy of this comparison.

In comparison to previous calculations, it is noted that in the OVGF calculations by Ohno *et al.*,²⁹ the symmetry of the first ionization bands switches from 2A_u for naphthalene to $^2B_{2g}$ for anthracene, which is in good agreement with the alternating lowest state symmetries in Figure 1 for acenes and Figure 3 for periacenes. Deleuze *et al.*³² have shown an accuracy in ionization energies within 0.02–0.07 eV for benzene through hexacene with extrapolations using CCSD(T) calculations combined with a focal point analysis⁶⁷ (FPA). A comparison of the raw data shows that our results agree well with the CCSD(T) results. Basis set extrapolations were not performed in this study since it requires correlation consistent basis sets instead of the Pople basis sets used here.

B. Electron affinity

Similar to the discussion of the most stable symmetries of the cationic states, the consequences of adding an electron to the LUNO is an alternation of the symmetry of the lowest state. Figure 4 (Table S4⁶⁶) indicates this phenomenon with a dotted line, pointing to the switching between the $^2B_{3g}$ and $^2B_{1u}$ states. The following aspects make the calculation of the electron affinities more difficult than those for the ionization energies: (i) the basis set effects are more pronounced than for the cationic systems and (ii) inclusion of the σ orbitals into the electron correlation scheme proved to be important.

The addition of the σ electrons to this system (independent of the basis and n) has a significant influence in the amount of ~0.73 eV in the average for $n = 2\text{--}5$ (see Table S5,⁶⁶ 6-31G basis). This value is approximately constant (Table S5⁶⁶); thus, 0.73 eV is taken for all values of n . Its use is denoted by the label +TC in the figures. For anthracene, as given in Table II, the addition of a diffuse function (aug-6-31G) to the π -only system increases the EA by 0.44 eV and the polarization (6-

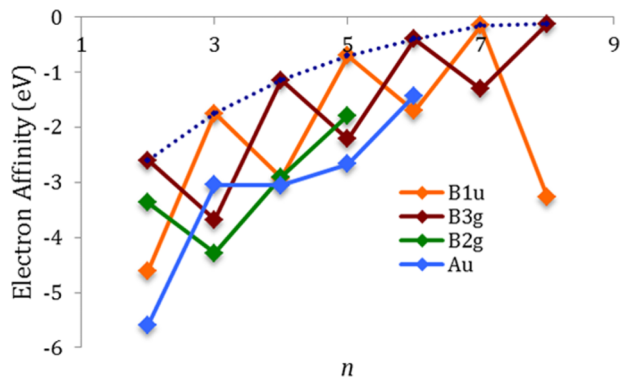


FIG. 4. Electron affinity for n -acenes ($n = 2\text{--}8$) for the π -MR-AQCC/RAS/CAS(4,4)/AUX/6-31G approach.

TABLE II. Basis set comparison with experiment for electron affinity (eV) for full valence calculations of anthracene.

Basis set	EA
6-31G	-0.98
6-31G(d)	-0.74
Aug-6-31G	-0.54
Aug-6-31G(d)	-0.29
d-aug-6-311G(d)	-0.17
d-aug-6-311G(2d)	-0.04
d-aug-6-311G(2d,f)	0.01
Experiment ^a	0.53

^aReference 27.

31G(d)) by 0.24 eV (both in reference to the $\pi/6\text{-}31G$). Table II shows that these effects are additive in that the aug-6-31G(d) gives an increase of 0.68 eV. The addition of a second diffuse function along with increased basis set flexibility in the s and p bases (d-aug-6-311G(d)) showed a 0.12 eV increase in EA upon the aug-6-31G(d) result. Including a second d function (d-aug-6-31G(2d)), an additional 0.13 eV is realized. The largest basis set used (d-aug-6-311G(2d,f)) adds a single f function to the d-aug-6-311G(2d) basis set for each of the carbons. This leads to an additional change of 0.05 eV.

The curve in Figure 5 labeled “Best Estimate” shows the combined effects of adding the σ correlation (0.73 eV) to the π system, two diffuse functions (0.56 eV), and three polarization functions (0.42 eV) (two in the d set and one in the f set), as taken from the anthracene data (Table II), which totals 1.71 eV. With this addition, the average theoretical-experimental error for the acene series is reduced to 0.44 eV, excluding the data point for naphthalene. Qualitatively, this “Best Estimate” curve gives the correct description of the anions, by virtue of being bound or unbound, for all acenes in the series in comparison to the experimental findings.^{26–28}

Table III shows the average difference and standard deviation (eV) between theory and experiment for electron affinities and first ionization energies of n -acenes for n in which experimental data are available. The input data for the statistical analysis are taken from Figures 2 and 5 for the ionization energy and electron affinity, respectively. As

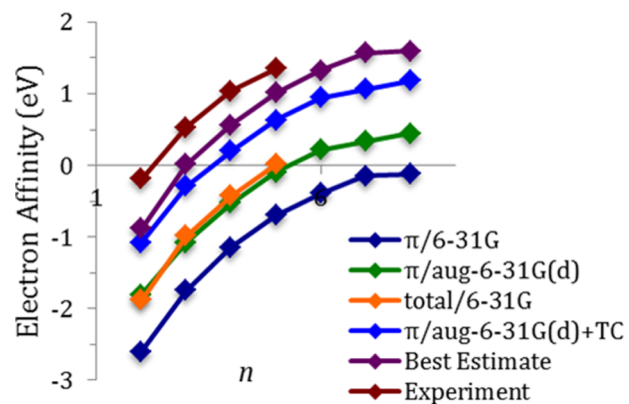


FIG. 5. Electron affinity for n -acenes ($n = 2\text{--}8$) for different basis sets and levels of theory as compared with experiment.^{26–28} TC denotes the approximate inclusion of σ correlation.

TABLE III. Average difference and standard deviation (eV) between theory and experiment for electron affinities and first ionization energies of n -acenes for n in which experimental data are available.

Method	Average \pm standard deviation
Ionization energy	
π -MR-AQCC/6-31G	0.52 ± 0.11
Total-MR-AQCC/6-31G	0.57 ± 0.10
Total-MR-AQCC/6-31G(2d)	0.33 ± 0.10
Best estimate	0.12 ± 0.04
Electron affinity	
π -MR-AQCC/6-31G	2.23 ± 0.15
π -MR-AQCC/aug-6-31G(d)	1.56 ± 0.08
Total-MR-AQCC/6-31G	1.50 ± 0.15
π -MR-AQCC/aug-6-31G(d)+TC	0.82 ± 0.08
Best estimate	$0.44^{\text{a}} \pm 0.15$

^a0.51 eV if naphthalene is included.

mentioned previously, *EA* calculations proved to be more sensitive to basis set effects and σ correlation than those of *IE*. This is evident when comparing the relative error between the basis sets. The π -MR-AQCC/6-31G, Total-MR-AQCC/6-31G, and Best Estimate data are available for direct comparison between the *IE* and *EA*.

Because of the size of the two-dimensional periacene systems, the calculations were limited to a π /MR-CISD+Q/6-31G approach. Results are displayed in Figure 6 (Table S6⁶⁶). As described for the acenes, an alternation between $^2\text{B}_{3g}$ and $^2\text{B}_{1u}$ is displayed by the dotted line in Figure 6. If the same *TC* correction of 0.73 eV as was obtained for the acenes is used also in a further approximation for the periacenes (shown as the upper dotted line in Figure 6), then all members of the series are bound or nearly bound. For the larger n values in the (3a, n) periacene series, positive *EA* values are obtained in any case. Their increase is, however, less pronounced than for the n -acenes (Figure 5).

In previous calculations, Rienstra-Kiracofe *et al.*³⁴ showed for 2-4 acenes that BLYP and B3LYP functionals with an aug-cc-pVDZ basis were especially useful for calculating VEA. They reported an average computational-experimental error of 0.18 eV. Modelli *et al.*³⁵ produce similar results with B3LYP/6-31+G*. Betowski *et al.*³⁶ extend this with B3LYP/6-31+G(d,p) and B3LYP/6-311G(d,p) to reach an

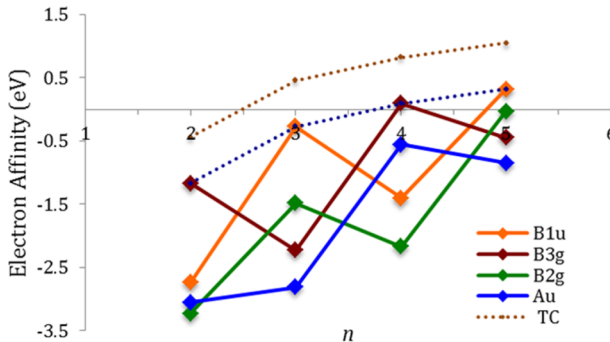


FIG. 6. Electron affinity for (3a, n) periacenes ($n = 2-5$) for the π -MR-CISD+Q/CAS(8,8)/6-31G approach. *TC* denotes the approximate inclusion of σ correlation.

average computational error of 0.07 eV. Going beyond DFT, CCSD(T) has been employed³⁷ up to an aug-cc-pVQZ basis sets with FPA⁶⁷ to extrapolate to the full basis limit giving AEAs of at most a 0.04 eV error. The CCSD(T) raw data points shown in Ref. 37 are only about 0.1 eV more accurate than our d-aug-6-31G(d)+TC data.

C. Radical character

It has been shown in several investigations that the primary contribution to the high radical character of graphene nanoribbons comes from its zigzag edge. Nakada *et al.*⁶⁸ showed analytically that there is a degenerate flatband near the Fermi level on the zigzag edge, which is not present on the armchair edge. Jiang *et al.*⁶⁹ went on to demonstrate that the carbon atoms on the zigzag edge of a graphene nanoribbon are more chemically reactive than those of a graphene sheet-, nanotube-, and nanoribbon armchair edge. Recently, the significance of the zigzag edge has also been reported by means of projected Hartree-Fock theory⁷⁰ and MR-AQCC calculations.^{18,38} The radical character of the system is examined via two means in this paper: the NO occupation and the effective number of unpaired electrons.

1. NO occupation

The NO occupations are derived from the spin-averaged one-electron density matrix, thus leading to a spectrum of occupation from zero to two. Though it was necessary to go beyond 6-31G to obtain more accurate electron affinities and ionization energies, NO occupations appear to be quite insensitive of basis set size. Although data are only available for anthracene for the largest basis sets, there is virtually no difference between π /6-31G and Total/6-311++G(2d,f)—orbital occupations agree within 0.02 e . Additionally, for the basis sets that are used for larger n -acenes (6-31G, 6-31G(d), 6-31G(2d), aug-6-31G(d), and aug-6-31G(2d)), a similar situation is found. In view of this good agreement and for reason of consistency with the periacene calculations, all figures here show data for π /6-31G. In Figure 7, the

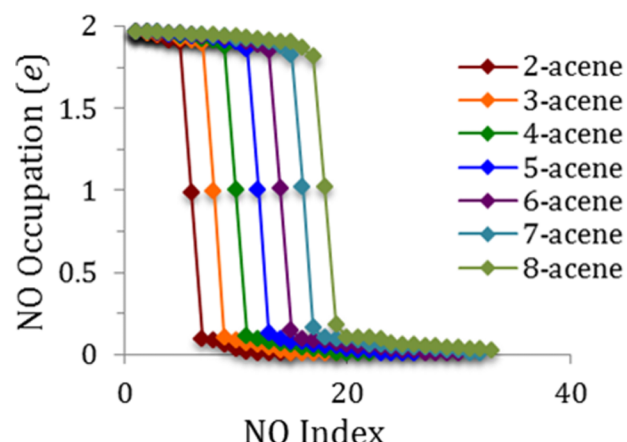


FIG. 7. NO occupations (e) for alternating cationic $^2\text{A}_u/ ^2\text{B}_{2g}$ states of n -acenes ($n = 2-8$) obtained from π -MR-AQCC/RAS/CAS(4,4)/AUX/6-31G calculations.

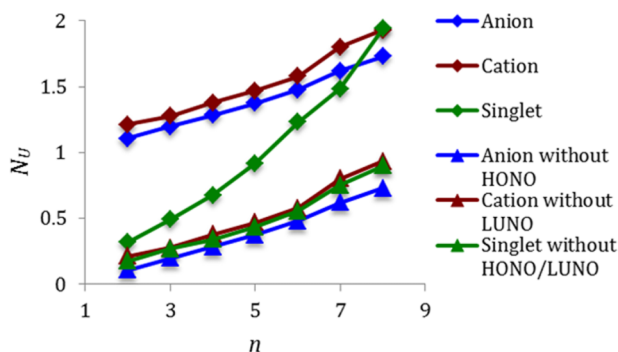


FIG. 8. Effective number of unpaired electrons for the $^1\text{A}_\text{g}$ (singlet), $^2\text{A}_\text{u}/^2\text{B}_\text{2g}$ (cation), and $^2\text{B}_\text{3g}/^2\text{B}_\text{1u}$ (anion) states of the n -acenes ($n = 2-8$) with and without the HONO and LUNO for the singlet and the single occupancy of the ions using the π -MR-AQCC/RAS/CAS(4,4)/AUX/6-31G method.

NO occupations for the cationic $^2\text{A}_\text{u}/^2\text{B}_\text{2g}$ series of n -acenes are shown. The NO occupation pattern for the remaining cases (anionic n -acenes, cationic, and anionic periacenes) is nearly identical and can be found in Figures S1-S3 of the supplementary material.⁶⁶

All of these graphs, as displayed in Figures 7 and S1-S3,⁶⁶ show a pronounced single radical character with only a slight increase in polyyradical character from the peripheral orbitals with increasing chain length. This polyyradical character coming from non-HONO/LUNO states is less pronounced to that of singlet¹⁸ and triplet³⁸ states found in previous MR-AQCC calculations.

2. Effective number of unpaired electrons

Figure 8 (Table S7⁶⁶) shows N_U values for the acenes computed using Eq. (2). It has been shown previously⁷¹ that, e.g., for a biradical formed from a dimer of the tetracyanoethylene anion, the N_U values can be well approximated from the HONO/LUNO orbitals exclusively. In the case of singlet and triplet graphene nanoribbons, it was found³⁸ that this model breaks down showing additional polyyradical character. To test the same behavior here, in Figure 8, N_U and reduced N_U values are shown, where the contributions from the nearly singly

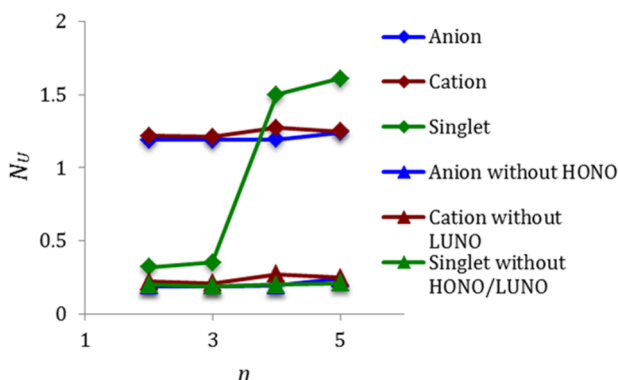


FIG. 9. Effective number of unpaired electrons for the $^1\text{A}_\text{g}$ (singlet), $^2\text{A}_\text{u}/^2\text{B}_\text{2g}$ (cation), and $^2\text{B}_\text{3g}/^2\text{B}_\text{1u}$ (anion) states of the $(3\text{a},\text{nz})$ periacenes ($n = 2-5$) with and without the HONO and LUNO for the singlet and the single occupancy of the ions using the π -MR-CISD/CAS(8,8)/6-31G method.

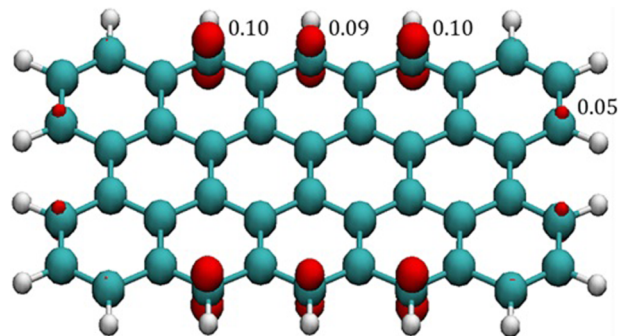


FIG. 10. Plot of the unpaired electron density for the anionic $^2\text{B}_\text{1u}$ state of the $(3\text{a},5\text{z})$ periacene (isovalue 0.005 e) of the π -MR-CISD/CAS(8,8)/6-31G calculation with individual atomic populations computed from a Mulliken analysis. $N_U = 1.25 \text{ e}$.

occupied NOs (for the singlet, this is the HONO and LUNO; for the doublets, it is the singly occupied NO) have been excluded. Figure 9 (Table S8⁶⁶) displays the corresponding graphs for the periacenes. Though the ionic species show singly radical character starting from 2-acene, they only show a gradual increase in unpaired electrons with increasing n , while the singlet (neutral) state for comparison increases rapidly. The reduced N_U values show for the ionic species of acenes a steady increase, which remarkably follows the singlet curve completely. This realization further supports the explanation given in Sec. III for the singly occupied orbital, in that only the HONO and LUNO orbital occupations were affected by the ionization and electron attachment. For the periacene series, Figure 9 shows that similar to the n -acene series, the N_U values of the neutral singlet case surpass the values of the ionic species with increasing chain length. Again, the reduced N_U values show a remarkable agreement between ionic and neutral cases. The constancy of these values with increasing n as compared to the observed increase in the n -acene series (Figure 8) is probably due to the use of the MR-CISD method in the former case. The dominance of the neutral systems in terms of N_U values for larger chains indicates a reduced chemical reactivity of the charged systems. This gives further support to the idea that neutral graphene possesses significant multiradical behavior as suggested previously,^{18,38} which can be reduced by adding/removing electrons such that only one open-shell orbital remains.

It has been shown^{15-20,38} that the bulk of the unpaired electron density for acenes and periacenes rests on the zigzag edge, thus leading to the conclusion it is the most reactive part of graphene. That is, the case presented here for the charged periacenes as well. Figures 10 and S4⁶⁶ show the unpaired density plots for the anionic and cationic species, respectively, for the $(3\text{a},5\text{z})$ periacene. Both ionic species show less radical character than the singlet state (Figure S5⁶⁶). The N_U values are $\sim 1.25 \text{ e}$ in the former and 1.61 e in the latter case.

IV. CONCLUSIONS

The purpose of this work was to explore the singly ionic states of graphene as a means to better understand its radical nature. This was accomplished by performing

high-level *ab initio* multiconfigurational and multireference calculations (MR-AQCC) on quasi-linear acenes and two-dimensional periacenes. The qualitative features of the character of the charged systems have been explained on the basis of removing/adding an electron to the HONO/LUNO system. Full valence calculations with extended basis sets were required to capture the effects of diffusivity and polarization of the ionic species. To make calculations at the multireference level possible for the whole range of *n*-acenes, a correction scheme for the effect of including the σ orbitals into the electron correlation process and using larger polarization basis functions was developed on the basis of extended calculations on anthracene and selected tests concerning their dependence on chain length. It was found that the main energetic trends in ionization energies and electron affinities could be quite well reproduced quantitatively on the basis of π -only electron correlation and a double zeta basis set. The remaining, non-negligible contributions could be determined very well from extended calculations for the acene series with the largest calculations being performed only for anthracene. It was found that contribution of sigma orbitals in the case of electron affinities and basis set effects was remarkably constant along the acene and periacene series, respectively. These findings certainly rely on error compensation when subtracting the total energies of the neutral and charged species. Nevertheless, this situation is consistent with the picture discussed in the context of unpaired densities that electron removal/addition can be discussed on the basis of HONO and LUNO. For this process and the concomitant polarization of the π system, a relatively small basis set is sufficient. The remaining bulk electron correlation effects seem to cancel. Even though it would of course be preferable to perform complete calculations including all valence electrons and a large basis set, the present results open the possibility to perform also useful, more limited calculations which can be focused on the multireference character of the wavefunction and the chemical reactivity following it.

This chemical aspect of our investigations is represented in the analysis of the natural orbitals and the unpaired density. Based on the comparison of total numbers of unpaired density, the calculations show that the ionic species should be less reactive than corresponding neutral singlet and triplet states. The analysis shows a singly occupied HONO and LUNO, respectively, being primarily responsible for the unpaired density. Starting with a zigzag length of four ($3a_1, 4z$) in the periacene series, the total unpaired density for the neutral singlet state surpasses the charged systems and continues to grow significantly. This comparison illustrates the prediction of the just-mentioned reduced reactivity of the latter systems. We expect similar stabilizing effects on doping graphene nanoribbons with heteroatoms.

ACKNOWLEDGMENTS

This work was supported by the National Science Foundation under Project No. CHE-1213263, by the Austrian Science Fund (SFB F41, ViCoM), and the Robert A. Welch Foundation under Grant No. D-0005. Shawn Horn is funded by a research fellowship at Texas Tech University. Computer

time at the Vienna Scientific Cluster (Project No. 70376) is gratefully acknowledged.

- ¹J. Jacob, *Pure Appl. Chem.* **68**, 301 (1996).
- ²K. Heymann, J. Lehmann, D. Solomon, M. W. I. Schmidt, and T. Regier, *Org. Geochem.* **42**, 1055 (2011).
- ³J. L. Weisman, T. J. Lee, F. Salama, and M. Head-Gordon, *Astrophys. J.* **587**, 256 (2003).
- ⁴X. Chilier, P. Boulet, H. Chermette, F. Salama, and J. Weber, *J. Phys. Chem.* **115**, 1769 (2001).
- ⁵F. Salama, *J. Mol. Struct.* **19**, 563-564 (2001).
- ⁶P. Brechignac and T. Pino, *Astron. Astrophys.* **343**, L49 (1999).
- ⁷K. S. Novoselov, D. Jiang, F. Schedin, T. Booth, V. V. Khotkevich, S. V. Morozov, and A. K. Geim, *Proc. Natl. Acad. Sci. U. S. A.* **102**, 10451 (2005).
- ⁸K. S. Novoselov, A. K. Geim, S. V. Morozov, D. Jiang, Y. Zhang, S. V. Dubonos, I. V. Grigorieva, and A. A. Firsov, *Science* **306**(5696), 666 (2004).
- ⁹A. K. Geim and K. S. Novoselov, *Nat. Mater.* **6**, 183 (2007).
- ¹⁰F. Banhart, J. Kotakoski, and A. V. Krasheninnikov, *ACS Nano* **5**, 26 (2011).
- ¹¹S. Niyogi, E. Belyarova, J. Hong, S. Khizroev, C. Berger, W. de Heer, and R. C. Haddon, *J. Phys. Chem. Lett.* **2**(19), 2487 (2011).
- ¹²S. D. Kahn, W. J. Hehre, and J. A. Pople, *J. Am. Chem. Soc.* **109**, 1871 (1987).
- ¹³C. L. Su and K. P. Loh, *Acc. Chem. Res.* **46**(10), 2275 (2013).
- ¹⁴D. Parviz, S. Das, H. S. T. Ahmed, F. Irin, S. Bhattacharia, and M. J. Green, *ACS Nano* **6**(10), 8857 (2012).
- ¹⁵D. Jiang and S. Dai, *J. Phys. Chem. A* **112**, 332 (2008).
- ¹⁶J. Hachmann, J. Dorando, M. Aviles, and G. Chan, *J. Chem. Phys.* **127**, 134309 (2007).
- ¹⁷G. Gidofalvi and D. Mazziotti, *J. Chem. Phys.* **129**, 134108 (2008).
- ¹⁸F. Plasser, H. Pasalic, M. H. Gerzabek, F. Libisch, R. Reiter, J. Burgdörfer, T. Müller, R. Shepard, and H. Lischka, *Angew. Chem., Int. Ed.* **52**, 2581 (2013).
- ¹⁹M. Bendikov, H. M. Duong, K. Starkey, K. N. Houk, E. A. Carter, and F. Wudl, *J. Am. Chem. Soc.* **126**, 7416 (2004).
- ²⁰O. Hod, V. Barone, and G. E. Scuseria, *Phys. Rev. B* **77**, 035411 (2008).
- ²¹J. E. Anthony, *Angew. Chem., Int. Ed.* **47**, 452 (2008).
- ²²Y. Gotkis, M. Oleinikova, M. Naor, and C. Lifshitz, *J. Phys. Chem.* **97**, 12282 (1993).
- ²³J. W. Hager and S. C. Wallace, *Anal. Chem.* **60**, 5 (1988).
- ²⁴D. Stahl and F. Maquin, *Chem. Phys. Lett.* **108**, 613 (1984).
- ²⁵E. Clar, J. M. Robertson, R. Schlogl, and W. Schmidt, *J. Am. Chem. Soc.* **103**, 1320 (1981).
- ²⁶P. D. Burrow, J. A. Michejda, and K. D. Jordan, *J. Chem. Phys.* **86**, 9 (1987).
- ²⁷J. Schiedt and R. Weintraub, *Chem. Phys. Lett.* **266**, 201 (1997).
- ²⁸L. Crocker, T. Wang, and P. Kebarle, *J. Am. Chem. Soc.* **115**, 7818 (1993).
- ²⁹M. Yamauchi, Y. Yamakita, H. Yamakodo, and K. Ohno, *J. Electron Spectrosc. Relat. Phenom.* **155**, 88-91 (1998).
- ³⁰V. Zakrzewski, O. Dolgounitcheva, and J. Ortiz, *J. Chem. Phys.* **105**, 8748 (1996).
- ³¹V. G. Zakrzewski, O. Dolgounitcheva, and J. V. Ortiz, *Int. J. Quantum Chem.* **80**, 836 (2000).
- ³²M. S. Deleuze, L. Claes, E. S. Kryachko, and J.-P. François, *J. Chem. Phys.* **119**, 3106 (2003).
- ³³M. Deleuze, *J. Chem. Phys.* **116**, 7012 (2002).
- ³⁴J. C. Rienstra-Kiracofe, C. J. Barden, S. T. Brown, and H. F. Schaefer III, *J. Phys. Chem. A* **105**, 524 (2001).
- ³⁵A. Modelli, L. Mussoni, and D. Fabbri, *J. Phys. Chem. A* **110**, 6482 (2006).
- ³⁶L. D. Betowski, M. Enlow, L. Riddick, and D. H. Aue, *J. Phys. Chem. A* **110**, 12927 (2006).
- ³⁷B. Hajgato, M. S. Deleuze, D. J. Tozer, and F. De Proft, *J. Chem. Phys.* **129**, 084308 (2008).
- ³⁸S. Horn, F. Plasser, T. Müller, F. Libisch, J. Burgdörfer, and H. Lischka, *Theor. Chem. Acc.* **133**, 1511 (2014).
- ³⁹P. G. Szalay, T. Müller, G. Gidofalvi, H. Lischka, and R. Shepard, *Chem. Rev.* **112**, 108 (2012).
- ⁴⁰P. G. Szalay and R. J. Bartlett, *Chem. Phys. Lett.* **214**, 481 (1993).
- ⁴¹I. Antol, M. Eckert-Maksic, H. Lischka, and Z. Maksic, *Eur. J. Org. Chem.* 3173 (2007).
- ⁴²E. B. Wang, C. A. Parish, and H. Lischka, *J. Chem. Phys.* **129**, 044306 (2008).
- ⁴³Z. H. Cui, H. Lischka, H. Z. Beneberu, and M. Kertesz, *J. Am. Chem. Soc.* **136**, 5539 (2014).
- ⁴⁴Z. H. Cui, H. Lischka, H. Z. Beneberu, and M. Kertesz, *J. Am. Chem. Soc.* **136**, 12958 (2014).

- ⁴⁵K. Takatsuka, T. Fueno, and K. Yamaguchi, *Theor. Chim. Acta* **48**, 175 (1978).
- ⁴⁶V. N. Staroverov and E. R. Davidson, *Chem. Phys. Lett.* **330**, 161 (2000).
- ⁴⁷M. Head-Gordon, *Chem. Phys. Lett.* **372**, 508 (2003).
- ⁴⁸C. Møller and M. S. Plesset, *Phys. Rev.* **46**, 618 (1934).
- ⁴⁹O. Vahtras, J. Almlöf, and M. W. Feyereisen, *Chem. Phys. Lett.* **213**, 514 (1993).
- ⁵⁰F. Weigend and M. Häser, *Theor. Chem. Acc.* **97**, 331 (1997).
- ⁵¹A. Schäfer, H. Horn, and R. Ahlrichs, *J. Chem. Phys.* **97**, 2571 (1992).
- ⁵²A. D. Becke, *Phys. Rev. A* **38**, 3098 (1988).
- ⁵³J. P. Perdew, *Phys. Rev. B* **33**, 8822 (1986).
- ⁵⁴M. Häser and R. Ahlrichs, *J. Comput. Chem.* **10**, 104 (1989).
- ⁵⁵O. Treutler and R. Ahlrichs, *J. Chem. Phys.* **102**, 346 (1995).
- ⁵⁶H. Dachsel, H. Lischka, R. Shepard, J. Nieplocha, and R. J. Harrison, *J. Comput. Chem.* **18**, 430 (1997).
- ⁵⁷H. Lischka, R. Shepard, R. M. Pitzer, I. Shavitt, M. Dallos, T. Mueller, P. Szalay, M. Seth, G. S. Kedziora, S. Yabushita, and Z. Zhang, *Phys. Chem. Chem. Phys.* **3**, 664 (2001).
- ⁵⁸T. Müller, *J. Phys. Chem. A* **113**, 12729 (2009).
- ⁵⁹H. Lischka, T. Müller, P. Szalay, I. Shavitt, R. M. Pitzer, and R. Shepard, *WIREs* **1**, 191 (2011).
- ⁶⁰H. Lischka, R. Shepard, I. Shavitt, R. Pitzer, M. Dallos, T. Müller, P. Szalay, F. Brown, R. Ahlrichs, H. Böhm, A. Chang, D. Comeau, R. Gdanitz, H. Dachsel, C. Ehrhardt, M. Ernzerhof, P. Höchtl, S. Irle, G. Kedziora, T. Kovar, V. Parasuk, M. Pepper, P. Scharf, H. Schiffer, M. Schindler, M. Schüler, M. Seth, E. Stahlberg, J.-G. Zhao, S. Yabushita, Z. Zhang, M. Barbatti, S. Matsika, M. Schuurmann, D. Yarkony, S. Brozell, E. Beck, J.-P. Blaudeau, M. Ruckenbauer, B. Sellner, F. Plasser, and J. Szymczak, COLUMBUS, an *ab initio* electronic structure program, release 7.0. (2012).
- ⁶¹W. L. Luken, *Chem. Phys. Lett.* **58**, 421 (1978).
- ⁶²W. J. Hehre, R. Ditchfield, and J. A. Pople, *J. Chem. Phys.* **56**, 2257 (1972).
- ⁶³R. Krishnan, J. S. Binkley, R. Seeger, and J. A. Pople, *J. Chem. Phys.* **72**, 650 (1980).
- ⁶⁴M. J. Frisch, J. A. Pople, and J. S. Binkley, *J. Chem. Phys.* **80**, 3265 (1984).
- ⁶⁵R. P. Hosteny, T. Dunning, Jr., R. R. Gilman, A. Pipano, and I. Shavitt, *J. Chem. Phys.* **62**, 4764 (1975).
- ⁶⁶See supplementary material at <http://dx.doi.org/10.1063/1.4906540> for tabulated ionization energies, electron affinities, total number of unpaired electrons and figures for NO occupations, and unpaired density plots.
- ⁶⁷N. L. Allinger, J. T. Fermann, W. D. Allen, and H. F. Schaefer III, *J. Chem. Phys.* **106**, 5143 (1997).
- ⁶⁸K. Nakada, M. Fujita, G. Dresselhaus, and M. S. Dresselhaus, *Phys. Rev. B* **54**, 17954 (1996).
- ⁶⁹D. Jiang, B. G. Sumpter, and S. Dai, *J. Chem. Phys.* **126**, 134701 (2007).
- ⁷⁰P. Rivero, C. A. Jimenez-Hoyos, and G. E. Scuseria, *J. Phys. Chem. B* **117**, 12750 (2013).
- ⁷¹Z. Cui, H. Lischka, T. Mueller, F. Plasser, and M. Kertesz, *Chem Phys Chem* **15**, 165 (2014).